Available online at www.sciencedirect.com
SCIENCE DIRECT
Biochemical and Biophysical Research Communications 338 (2005) 175–190
BBRC
www.elsevier.com/locate/ybbrc

Review

Rieske business: Structure–function of Rieske non-heme oxygenases

Daniel J. Ferraro, Lokesh Gakhar, S. Ramaswamy *

Department of Biochemistry, University of Iowa Roy J. and Lucille A. Carver College of Medicine, 51 Newton Road, 4-403 BSB, Iowa City, IA 52242, USA

Received 16 July 2005
Available online 8 September 2005

Abstract

Rieske non-heme iron oxygenases (RO) catalyze stereo- and regiospecific reactions. Recently, an explosion of structural information on this class of enzymes has occurred in the literature. ROs are two/three component systems: a reductase component that obtains electrons from NAD(P)H, often a Rieske ferredoxin component that shuttles the electrons and an oxygenase component that performs catalysis. The oxygenase component structures have all shown to be of the α_3 or $\alpha_3\beta_3$ types. The transfer of electrons happens from the Rieske center to the mononuclear iron of the neighboring subunit via a conserved aspartate, which is shown to be involved in gating electron transport. Molecular oxygen has been shown to bind side-on in naphthalene dioxygenase and a concerted mechanism of oxygen activation and hydroxylation of the ring has been proposed. The orientation of binding of the substrate to the enzyme is hypothesized to control the substrate selectivity and regio-specificity of product formation.

Keywords: Rieske iron–sulfur center; Non-heme iron enzyme; Dioxygen binding; Rieske oxygenase; Reaction mechanism; Gating; Regiospecificity; Dioxygenase

Rieske beginnings: Introduction

Evidence for microbial metabolism of aromatic hydrocarbons has been present in the literature for many years. However, enzymes, now known as Rieske non-heme iron oxygenases (ROs)[1], were not known until 1968 [1,2]. These enzymes are responsible for the generation of *cis*-dihydroxylated metabolites, a common first step in the bacterial degradation of many aromatic compounds. Gibson et al.'s [2] work with arene metabolizing strains of *Pseudomonas putida* showed the formation of a *cis*-benzene glycol intermediate in the formation of catechol, leading them to propose the mechanism of *cis*-dihydroxylation in the metabolism of arenes. Molecular oxygen was identified as the source of the hydroxy moieties on the products, and NAD(P)H was identified as the reductant [3]. This mechanism differed from the known mechanism for the formation of dihydrodiols in mammalian cells, usually performed by P450 monooxygenase systems [4]. Strains of *Pseudomonas* were identified that formed optically pure (+)-*cis*-(1*R*,2*S*)-dihydroxy-1,2-dihydronaphthalene from naphthalene [4,5] and (+)-*cis*-1,2-dihydroxy-3-methylcyclohexa-3,5-diene from toluene [6,7]. The enzymes responsible for the conversion of these substrates were later identified, respectively, as the three-component naphthalene dioxygenase and toluene dioxygenase RO systems (Fig. 1).

Identification and purification of the individual components allowed for more detailed studies of RO enzyme systems, including experiments to determine the atomic structures of each component. In this review, we discuss (a) the current body of structural work on ROs, (b) how this information has played a role in understanding the mechanism of addition of molecular oxygen to substrate, and (c) how structural information is used to predict substrate specificity, and regio- and stereo-selectivity of product formation.

* Corresponding author. Fax: +1 319 335 9570.
E-mail address: s-ramaswamy@uiowa.edu (S. Ramaswamy).
[1] In this review, RO will refer to the enzyme system, such as NDO for naphthalene dioxygenase system.

0006-291X/$ - see front matter © 2005 Elsevier Inc. All rights reserved.
doi:10.1016/j.bbrc.2005.08.222

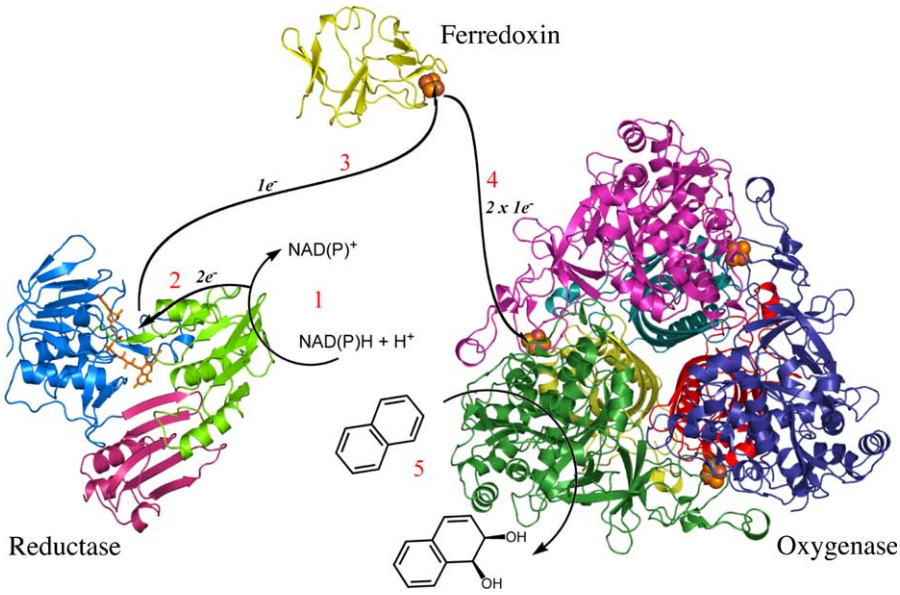

Fig. 1. The three components of a Rieske oxygenase system. (1) The reductase (BPDO-R_{KKS102} shown in figure) oxidizes NAD(P)H to $NADP^+$ at the NAD(P)H binding site, capturing 2 electrons. (2) The electrons are stored on the flavin until (3) the reductase completes a 1 electron reduction of the ferredoxin component (BPDO-F_{LB400} shown in figure). (4) The ferredoxin shuttles the electron received from the reductase to the oxygenase Rieske cluster (BPDO-O_{RHA1} shown in figure). This step occurs twice for (5) each molecule of product formed at the mononuclear iron site. The flavin is shown as a stick representation, the Rieske cluster and mononuclear iron are shown as spheres.

Rieske nature: The Rieske cluster

Many examples of iron–sulfur clusters exist in nature; frequently these appear in proteins involved in electron transport. In these proteins, the iron–sulfur cluster is involved in the storage of electrons. There are multiple types of iron–sulfur clusters and they are grouped into the following categories based on their atomic content: [2Fe–2S], [3Fe–4S], [4Fe–4S], and other hybrid or mixed metal types [8]. Two general types of [2Fe–2S] clusters are known and they differ in their coordinating residues. The plant-type and adrenodoxin [2Fe–2S] clusters are coordinated to the protein by four cysteine residues.[2] The Rieske-type [2Fe–2S] cluster is coordinated to its protein by two cysteine residues and two histidine residues [9,10]. Rieske-type iron–sulfur clusters are common to non-heme iron oxygenase systems such as the naphthalene, toluene, and biphenyl dioxygenase systems as well as other redox proteins, such as spinach chloroplast b_6f and cytochrome bc_1 [8].

In Rieske cluster containing proteins, one iron of the Rieske cluster, Fe_1, is coordinated by two histidines while the other iron, Fe_2, is coordinated by two cysteines (Fig. 2). Two inorganic sulfide ions bridge the two iron ions forming a flat, rhombic cluster. The two sulfide ions of the cluster hydrogen bond with the main-chain nitrogens [11]. The iron ligated to the cysteines remains in a ferric state, regardless of the reduction state of the cluster, while the histidine-ligated iron goes from a ferric state to a ferrous state when reduced [12–15]. Two kinds of Rieske type [2Fe–2S] clusters are found in enzymes, high reduction potential and low reduction potential. The high reduction potential Rieske cluster proteins have reduction potentials of +150 to +490 mV and include the cytochrome bc_1 and b_6f complexes. The low redox potential enzymes have a reduction potential of −150 to −50 mV and include the ROS enzymes [16]. Although there is a large variation in reduction potentials, the overall structures of Rieske cluster-binding domains are very similar. There is still debate as to what structural features contribute to an enzyme's reduction potential; however, hydrogen bonding networks [17–19] and polypeptide dipoles [20] have been suggested to play a role.

Rieske design: Rieske non-heme iron oxygenase systems

Rieske non-heme iron oxygenase systems form a soluble electron transport chain to harness the reductive power of NAD(P)H and activate molecular oxygen. Depending on the system, two or three separate protein components are involved in the movement of an electron from NAD(P)H to O_2: a reductase, a ferredoxin (in 3 component systems), and an oxygenase (Fig. 1). In this review, RO components will be abbreviated using the following convention: $XO\text{-}Y_Z$, where XO is the oxygenase system, Y is R, F, or O and represents the reductase, ferredoxin or oxygenase component, respectively, and Z is the strain designation from which the enzyme system was originally isolated. We have chosen to use strain designation rather than species to avoid confusion caused by reclassification of some bacterial species after RO systems have been isolated, characterized, and classified. Reductase (RO-R) enzymes are classified into

[2] The plant-type and adrenodoxin-type [2Fe–2S] clusters have been grouped together for this review and will be referred to collectively as plant-type [2Fe–2S] clusters.

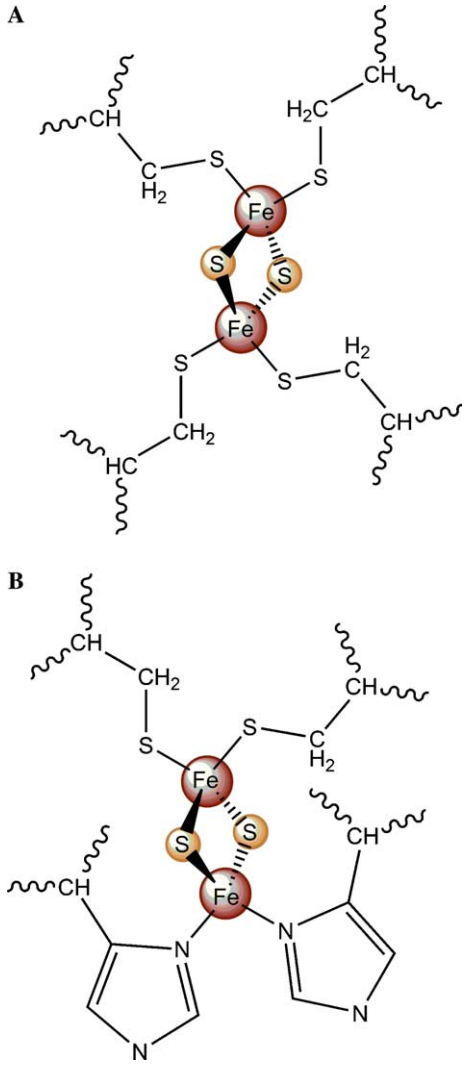

Fig. 2. Diagrams of plant-type and Rieske-type [2Fe–2S] iron–sulfur clusters. (A) Plant-type clusters are coordinated by 4 cysteines, while (B) Rieske-type clusters are coordinated by 2 cysteines and 2 histidines.

two separate structural families: ferredoxin-NADP reductase (FMN) and glutathione reductase. The FMN family reductases exhibit structural similarity to other plant ferredoxin reductases and contain an FAD or FMN-binding domain, an NADH-binding domain, and a plant-type [2Fe–2S] cluster domain. Structures of FMN family RO-R enzymes, phthalate dioxygenase reductase (PDO-R_{PHK}) from *Pseudomonas cepacia* strain PHK [21] and benzoate dioxygenase reductase (BZDO-R_{ADP1}) from *Acinetobacter baylyi* strain ADP1 [22], have been determined (Fig. 3). The glutathione reductase family reductases are structurally similar to enzymes such as dihydrolipoamide dehydrogenases and thioredoxin reductases. Glutathione reductase family RO-R enzymes contain three domains: an FAD-binding domain, an NADH-binding domain, and a C-terminal domain. The structure of biphenyl dioxygenase reductase (BPDO-R_{KKS102}) from *Pseudomonas* sp. strain KKS102, an RO-R enzyme from the glutathione reductase family has been determined [23]. Lee et al. [24] have reported the crystallization of another glutathione reductase-type reductase, toluene dioxygenase reductase (TDO-R_{F1}) from *P. putida* strain F1.

The ferredoxin (RO-F) component is present in three-component RO systems and carries an electron from the RO-R to the terminal oxygenase (RO-O) component. These small proteins contain either a plant-type [2Fe–2S] or Rieske-type [2Fe–2S] cluster. The structures of biphenyl dioxygenase ferredoxin (BPDO-F_{LB400}) from *Burkholderia xenovorans* strain LB400 [25], naphthalene dioxygenase ferredoxin (NDO-$F_{9816\text{-}4}$) from *Pseudomonas* sp. strain NCIB 9816-4 [26] carbazole dioxygenase ferredoxin (CARDO-F_{CA10}) from *Pseudomonas resinovorans* strain CA10 [27] and biphenyl dioxygenase reductase (BPDO-F_{B1}) from *Sphingomonas yanoikuyae* strain B1 (Brown and Yu, Personal Communication), all containing Reiske-type [2Fe–2S] clusters, have been determined (Fig. 3). Lee et al. [24] has also reported the crystallization of toluene dioxygenase ferredoxin (TDO-F_{F1}) from *P. putida* strain F1.

The α-subunit of the RO-O enzyme can be divided into the Rieske [2Fe–2S] cluster domain and the mononuclear iron-containing catalytic domain. The Rieske cluster accepts electrons from the reductase or ferredoxin and passes them on to the mononuclear iron for catalysis. The mononuclear iron is part of the predominantly hydrophobic active site and comprised of the C-terminal portion of the protein and the first ~40 residues of the N-terminal sequence. This domain is a mix of helices and strands forming a TBP-like or helix-grip fold and is a member of the Bet v1-like superfamily [28]. At this time, structures for eight unique RO-O enzymes have been determined (Fig. 4). These include naphthalene dioxygenase (NDO-$O_{9816\text{-}4}$) from *Pseudomonas* sp. strain NCIB 9816-4 [11,29–33], biphenyl dioxygenase (BPDO-O_{RHA1}) from *Rhodococcus* sp. strain RHA1 [34], biphenyl dioxygenase (BPDO-O_{B1}) from *S. yanoikuyae* strain B1 (Ferraro, unpublished), naphthalene dioxygenase (NDO-O_{12038}) from *Rhodococcus* sp. strain NCIMB 12038 [35], nitrobenzene dioxygenase (NBDO-O_{JS765}) from *Comamonas* sp. strain JS765 [36], cumene dioxygenase (CDO-O_{IP01}) from *P. fluorescens* strain IP01 [37], 2-oxoquinoline monooxygenase (OMO-O_{86}) from *P. putida* strain 86 [38], and carbazole-1,9α-dioxygenase (CARDO-O_{CA10}) from *P. resinovorans* strain CA10 [39]. Lee et al. [24] also reports the crystallization of toluene-2,3-dioxygenase (TDO-O_{F1}). While sequences of these enzymes vary substantially, the known structures are well conserved.

Some RO-O enzymes contain an α- and a β-subunit. The β-subunit is structurally similar to the enzyme scytalone dehydratase [40] and nuclear transport factor [41]. It is believed that the purpose of the β-subunit is purely structural for enzymes such as NDO-$O_{9816\text{-}4}$ and NBDO-O_{JS765} [11,36]; however, there are reports that suggest the β-subunits of some RO-O enzymes can influence substrate [42]. OMO-O_{86} and CARDO-O_{CA10} contain only α-subunits [38,39]. In these structures, loops on the α-subunits may of-

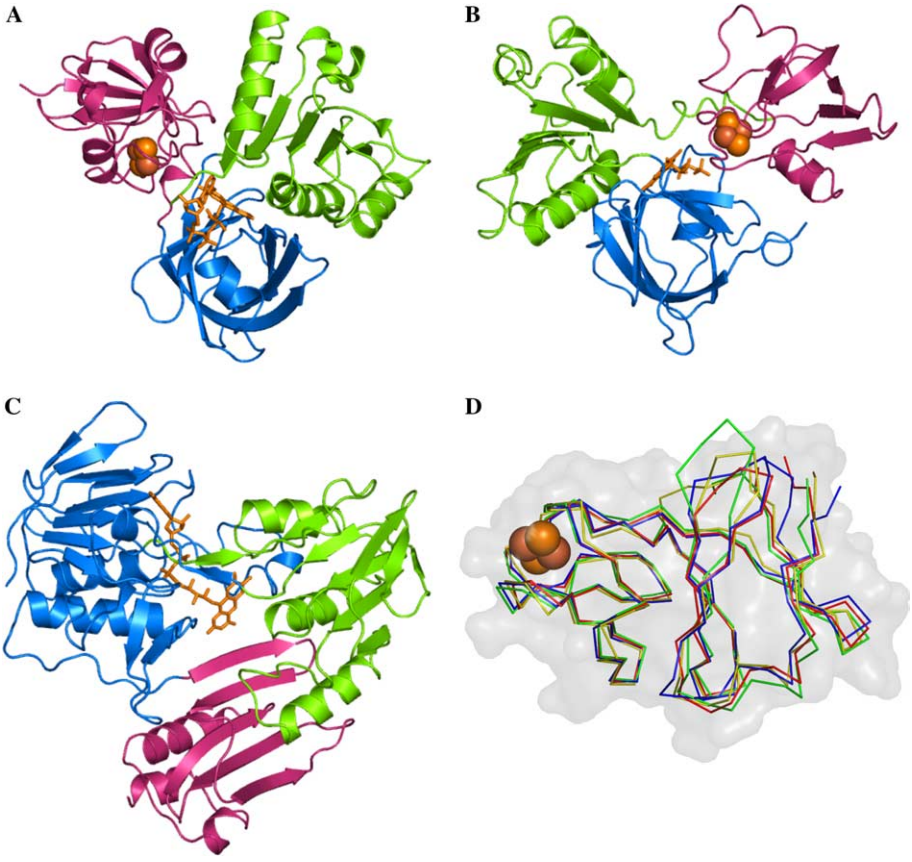

Fig. 3. Structures of RO-R and RO-F enzymes. Cartoon representations of the three different types of RO-R enzymes known to date. (A) BZDO-R_{ADP1} is a class IB FMN-type reductase and contains a FAD-binding domain, a NADH-binding domain and a plant-type [2Fe–2S] iron–sulfur cluster. (B) PDO-R_{PHK} is a class IA FMN-type reductase. (C) BPDO-R_{KKS102} is a class IIB glutathione reductase-type reductase. The flavins are shown as sticks and the Rieske cluster as spheres. (D) An overlay of BPDO-F_{LB400} (yellow), NDO-$F_{9816\text{-}4}$ (red), CARDO-F_{CA10} (green) and BPDO-F_{B1} (blue).

fer increased stability, removing the need for a stabilizing β-subunit. Structures of RO-O enzymes determined to date have all demonstrated an α_3 or $\alpha_3\beta_3$ mushroom-shaped quaternary structure with three-fold symmetry. In all of the known structures of ROs, the Rieske cluster and mononuclear iron within a single α-subunit are too far apart for electron transfer (~45 Å); however, the quaternary arrangement of the monomers places the Rieske cluster and mononuclear iron of separate subunits within ~12 Å, a reasonable distance for electron transfer (Fig. 5). Phthalate dioxygenase has been reported in the past to have an α_4 quaternary arrangement; however, this has been a point of dispute. The α_4 quaternary arrangement also suggests a different model for electron transport. Previous studies of NDO-$O_{9816\text{-}4}$ [43] and NDO-O_{12038} [44] enzymes originally suggested a quaternary structure other than $\alpha_3\beta_3$; however, subsequent structural work demonstrated that their quaternary structure was $\alpha_3\beta_3$. Recent structural work with the α-only dioxygenases OMO-O_{86} [38] and CARDO-O_{CA10} [39] have shown the quaternary structure to be an α_3 trimer with similar Rieske-mononuclear domain interactions. These results suggest that phthalate dioxygenase may also be an α_3 trimer with a similar geometric arrangement between neighboring Rieske and mononuclear iron positions.

ROs have historically been classified by their components (Table 1). This classification method groups ROs by the type of iron–sulfur cluster contained in the reductase, the presence of FMN or FAD, and the type of iron–sulfur cluster contained in the ferredoxin component, if present [45,46]. A second method of organization places ROs into families based on substrate specificity profiles and phylogenetic trees [47,48]. This classification emphasizes the structure–function relationship of the RO-O α-subunit; however, some ROs are outliers in this scheme (Table 2). A third, more inclusive scheme has been developed that classifies ROs based on the oxygenase component sequence identity [49].

Rieske behavior: Structural insight on RO function

The mechanism of oxygen addition to substrate by ROs has been studied structurally using NDO-$O_{9816\text{-}4}$ as a model system. The mechanism of ROs has been reviewed previously [50–56]. Single turnover studies with $NDO_{9816\text{-}4}$ demonstrated that the oxygenase component was necessary and sufficient for the oxidation of naphthalene to *cis*-(1*R*,2*S*)-dihydroxy-1,2-dihydronaphthalene [57]. The oxygenase component of the 2-component benzoate dioxygenase system

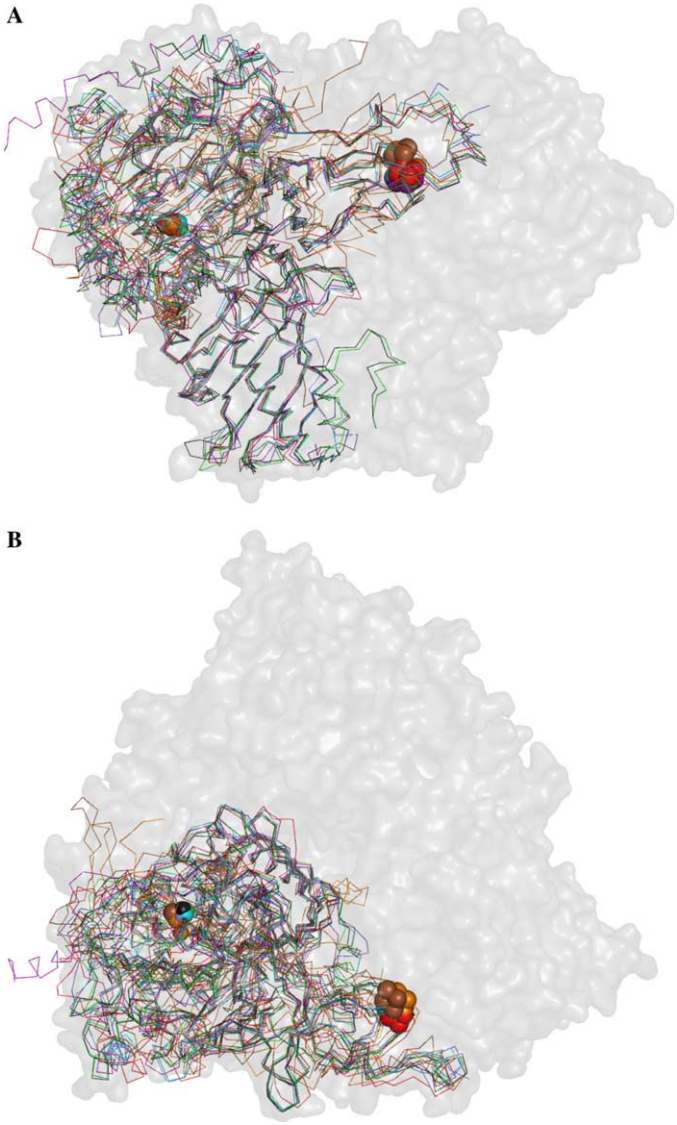

Fig. 4. Overlays of the α- and β-subunits of RO-O enzymes. (A) Side view and (B) top view perspectives showing the general volume of the mushroom-shape of the oxygenase component. Overlaid inside the surface shell are the α- and β- (A only) subunits. The structures of the α-subunits are highly conserved in the N-terminal portion of the protein containing the Rieske cluster-binding domain. More variability is seen near the mononuclear iron-binding site. The structures of the β-subunits are highly conserved despite low sequence homology. Colors for each RO-O are as follows: black, NDO-$O_{9816\text{-}4}$; purple, BPDO-O_{B1}; green, NBDO-O_{JS765}; brown, CARDO-O_{CA10}; slate, CDO-O_{IP01}; cyan, BPDO-O_{RHA1}; red, NDO-O_{12038}, and orange, OMO-O_{86}.

has also been shown to be necessary and sufficient for the dihydroxylation of benzoate [58]. The current model of oxygen addition can be broken into two major steps: (a) activation of molecular oxygen and (b) addition of oxygen to substrate in a specific manner. The mechanism of oxygen activation has been studied in greater detail through structural methods than substrate specificity or selectivity of product formation. Also, it is believed that oxygen is activated in the same manner by the enzyme regardless of the substrate. The remainder of this review will address structure–function relationships in RO-O enzymes.

Rieske moves: Structural information on RO oxygen activation

Rieske cluster—electron gateway

In three-component systems, the oxygenase Rieske cluster accepts the electrons from the ferredoxin; in two-component systems, the oxygenase accepts electrons directly from the reductase component. The electron then travels from the Rieske cluster to the mononuclear iron to be used in catalysis. Structures of NDO-$O_{9816\text{-}4}$ with oxidized and reduced Rieske clusters have been solved, respectively, to 2.2 and 1.7 Å [32]. No difference in bond length or overall structure of the Rieske cluster was seen at this resolution. Extended X-ray absorption fine structure (EXAFS) studies of other RO-O enzymes have shown a very small but distinct change in the bond lengths between the iron and sulfide ions of the Rieske cluster when reduced [16,59]. A larger bond length change has been observed between the imidazole nitrogens and iron ions, lengthening 0.1 Å upon reduction [16].

Subunit interface—aspartic acid bridge

Although the mononuclear iron and Rieske cluster within one α-subunit are ~45 Å apart, the mononuclear iron of one subunit is ~12 Å away from the adjacent Rieske cluster in the quaternary structure. This allows room for a "bridge" between the Rieske cluster of one subunit and the active site mononuclear iron in the neighboring subunit. In NDO-$O_{9816\text{-}4}$, Asp205 hydrogen bonds to both His205, a ligand to the mononuclear iron, and His104, a ligand to the Rieske [2Fe–2S] cluster. To determine the function of Asp205, several mutants were constructed and screened for activity [60]. Iron incorporation into Asp205 mutants did not differ from wild-type, as determined by UV/vis and EPR spectra. Although there were no changes in the spectral properties or content of the iron in the enzyme when Asp205 was mutated, the catalytic activity was greatly diminished or not detected. The authors concluded that Asp205 might be acting as a path for electron transfer. The analogous residue in anthranilate dioxygenase oxygenase, Asp218, has also been studied [61]. Loss of function was also seen in Asp218 mutants; in addition, an approximately −100 mV shift in redox potential of the Rieske cluster was detected. This shift was caused by the inability to protonate the Rieske cluster-coordinating histidine, which was a result of the loss of a stabilizing hydrogen bond with Asp218.

A study of 2-oxoquinoline monooxygenase (OMO-O_{86}) showed a change in the position of Asp218 and formation of a hydrogen bond with the Rieske-coordinated His108 upon reduction of the Rieske cluster [38]. This aspartate side chain lies in the subunit interface and is structurally analogous to Asp205 in NDO-$O_{9816\text{-}4}$. The large position change of Asp218 upon Rieske cluster reduction suggests the creation of a hydrogen bond. The reduction-coupled

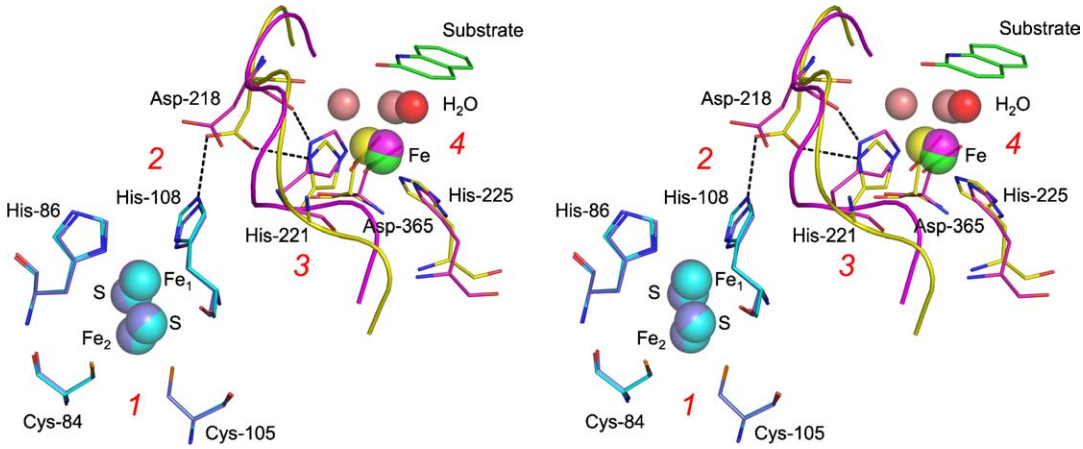

Fig. 5. The Rieske–mononuclear interface in OMO-O_{86}. The Rieske cluster and mononuclear iron in an individual RO-O α-subunit are ~45 Å apart. The quaternary structure of RO-O enzymes allow the Rieske cluster and mononuclear iron to come within ~12 Å, allowing electron transfer between sites. This scheme also depicts the redox-dependent structural changes seen in OMO-O_{86} believed to be integral to the mechanism of RO-O oxygen activation. (1) When the Rieske cluster is reduced, (2) protonation of the Rieske-coordinating histidine occurs. Redox-dependent protonation allows for a hydrogen bond to form between His108 and Asp218, and (3) induces a conformational change in the interface helix. This conformational change causes a geometric rearrangement at the mononuclear iron (4) changing the iron from tetragonal to a pentagonal/distorted octahedral geometry. The pentagonal/distorted octahedral geometry at the mononuclear iron allows for two water ligands (pink), rather than a single water ligand (red) seen in the tetragonal form. The two-ligand (pink) geometry has been suggested to have a higher affinity for O_2 than the one-ligand (red) and would also allow side-on binding required for catalysis. The substrate, 2-oxoquinoline, is shown in green.

protonation of His108 creates a hydrogen bond donor not present in the oxidized Rieske cluster structure. This change also induces a geometric rearrangement at the mononuclear iron site due to the movement of the interface helix. His221, also on the interface helix, coordinates the mononuclear iron, which has tetrahedral coordination geometry in the oxidized state. In this state, the fourth ligand is a single water (hydroxyl) molecule. When reduced, His221 shifts closer to the other two coordinating side chains, allowing for a fifth position in the coordination sphere. This five-coordinate geometry is suggested to be more conducive for oxygen binding and subsequent activation [38] (Fig. 5). The structural information also links the protonation of the Rieske cluster-coordinating histidine with higher oxygen affinity for the mononuclear iron when the Rieske cluster is reduced [61].

Mononuclear iron—catalytic scaffold

The mononuclear iron coordination in NDO is an example of the 2-His-1-carboxylate facial triad motif found in many non-heme iron enzymes [62]. This motif has been shown to be a common way for enzymes to incorporate an iron(II) catalytic site in proteins for use in a wide variety of reactions. Reactions carried out by heme iron-containing enzymes, such as monohydroxylation or epoxidation, can also be carried out by non-heme 2-His-1-carboxylate facial triad enzymes. This type of coordination at the mononuclear site of Rieske dioxygenases leaves the face of the iron exposed to the large, hydrophobic active site, creating a catalytic platform where oxygen can bind and subsequently react with substrate to form product through a variety of reactions [63]. This allows the iron to have up to three exogenous ligands bind to the iron. Therefore, these enzymes are able to perform much more complicated reactions than heme iron enzymes, such as oxidative ring closure, desaturation, oxidative catechol cleavage, and arene-*cis*-dihydroxylation [53].

A unique feature of these enzymes is the ability to bind molecular oxygen (O_2) side-on to the iron. Side-on binding of O_2 has been proposed as a possible transition state in the mechanism of NDO-$O_{9816\text{-}4}$ [55]. Crystallographic models of Rieske oxygenases show O_2 bound to the iron in a side-on fashion when in a binary complex with substrate [32,37]. The side-on binding of O_2 allows each oxygen to attack neighboring carbons from the same face of the arene, producing a *cis*-dihydrodiol. Nitric oxide (NO), an O_2 analog, has been shown to behave differently from O_2 at the active site. Crystallographic models of NDO-$O_{9816\text{-}4}$ with NO bound to the mononuclear iron show NO bound end-on to the mononuclear iron in the presence of substrate [33]. In the absence of the substrate, NO binds to a hydrophobic pocket in the substrate-binding cavity. Hence, it is possible that O_2 binds the same hydrophobic pocket before binding to the mononuclear iron.

As mentioned earlier, coordination of the mononuclear iron is coupled to the redox state of the Rieske cluster, exemplified by the tetragonal and distorted octahedral coordination seen in OMO-O_{86} [38]. A distorted octahedral coordination at the mononuclear site is also seen in crystal structures of NDO-$O_{9816\text{-}4}$ bound to dihydrodiol product. The redox-coupled geometric rearrangement seen at the mononuclear iron has been suggested to control end-on versus side-on binding of oxygen and possibly alteration of O_2 affinity [38]. Allosteric control of substrate binding has been shown to extend to aromatic substrate. Studies

Table 1
Classification scheme based on RO components

System	Class	Reductase	Ferredoxin	Oxygenase	Example	Structures		
						Reductase	Ferredoxin	Oxygenase
Two component	IA	FMN $[2Fe–2S]_P$		$[2Fe\text{-}2S]_R$ Fe^{2+}	Pthalate dioxygenase	$PDO\text{-}R_{PHK}$		
	IB	FAD $[2Fe–2S]_P$		$[2Fe–2S]_R$ Fe^{2+}	Benzoate dioxygenase, 2-oxoquinoline monooxygenase	$BZDO\text{-}R_{ADP1}$	$OMO\text{-}F_{86}$	
Three component	IIA	FAD	$[2Fe–2S]_P$	$[2Fe–2S]_R$ Fe^{2+}	Dibenzofuran dioxygenase			
	IIB	FAD	$[2Fe–2S]_R$	$[2Fe–2S]_R$ Fe^{2+}	Toluene dioxygenase, biphenyl dioxygenase, cumene dioxygenase	$BPDO\text{-}R_{KKS102}$	$BPDO\text{-}F_{LB400}$	$BPDO\text{-}O_{B1}$, $BPDO\text{-}O_{RHA1}$, $CDO\text{-}O_{IP01}$, $OMO\text{-}O_{86}$
	III	FAD $[2Fe–2S]_R$	$[2Fe–2S]_R$	$[2Fe–2S]_R$ Fe^{2+}	Naphthalene dioxygenase, 2-nitrotoluene dioxygenase, nitrobenzene dioxygenase, carbazole dioxygenase		$NDO\text{-}F_{9816\text{-}4}$, $CARDO\text{-}F_{CA10}$	$NDO\text{-}O_{9816\text{-}4}$, $NBDO\text{-}O_{JS765}$, $NDO\text{-}O_{12038}$, $CARDO\text{-}O_{CA10}$

$[2Fe–2S]_P$, plant-type iron–sulfur cluster.
$[2Fe–2S]_R$, Rieske type iron–sulfur cluster.

Table 2
Classification scheme based on RO families

Rieske non-heme oxygenase family	Example substrates	Example members	Structures		
			Reductase	Ferredoxin	Oxygenase
Naphthalene	Naphthalene, indole, nitroarenes, phenanthrene	Naphthalene dioxygenase, nitrobenzene dioxygenase		$NDO\text{-}F_{9816\text{-}4}$	$NDO\text{-}O_{9816\text{-}4}$, $NBDO\text{-}O_{JS765}$, $NDO\text{-}O_{12038}$
Toluene/biphenyl	Toluene, cumene, biphenyl, PCBs, benzene	Benzene dioxygenase, toluene dioxygenase, biphenyl dioxygenase, cumene dioxygenase	$BPDO\text{-}R_{KKS102}$	$BPDO\text{-}F_{LB400}$	$BPDO\text{-}O_{RHA1}$, $BPDO\text{-}O_{B1}$, $CDO\text{-}O_{IP01}$
Benzoate	Benzoate, toluate	Benzoate dioxygenase	$BZDO\text{-}R_{ADP1}$		
Phthalate	Phthalate	Phthalate dioxygenase, 2-oxoquinoline8-monooxygenase	$PDO\text{-}R_{PHK}$		$OMO\text{-}O_{86}$

CARDO components do not fit well into this classification system.

of the position of naphthalene and toluene bound to NDO-$O_{9816\text{-}4}$ in both the resting state and the fully reduced state have been performed using ENDOR spectroscopy [64–66]. These studies show that the substrate moves approximately 0.5 Å away from the mononuclear iron when the Rieske cluster changes from the oxidized to reduced state. The movement of substrate away from the iron when the Rieske cluster is reduced may also act as a physical mechanism of gating oxygen reactivity [64].

The RO–O mononuclear iron is labile and the oxidized form is more easily removed than the reduced. In vitro enzyme activity studies have also shown that the addition of ferrous iron can increase turnover [67–69]. This is believed to help saturate the mononuclear active site after some iron is lost in purification [58,66]. More subtle changes in the position of the mononuclear iron have been observed. Structures of NDO-$O_{9816\text{-}4}$ bound to NO show the mononuclear iron shifted to a different position as compared to structures of NDO-$O_{9816\text{-}4}$ with water bound to the mononuclear iron [33]. Shifts in the mononuclear iron position are also seen in structures of OMO-O_{86} [38]. It is believed that these shifts may play a role in the catalytic mechanism.

There is a controversy on the oxidation states that the iron goes through during catalysis. Some reports suggest that O_2 activation at RO-O mononuclear sites happens through Fe(IV) and Fe(V) states [56,57,70]. However, our preferred hypothesis is that gating occurs to control the flow of the second electron from the Rieske cluster and that no higher order oxidation states need be invoked for a concerted mechanism leading to *cis*-dihydroxylation reactions catalyzed by RO-O enzymes. This mechanism would involve the formation of an iron(III)–(hydro)peroxo complex and is supported by our observation of side-on binding of oxygen to iron [32,37], uncoupling of substrate turnover, and production of H_2O_2 [71], demonstration of a peroxide shunt in formation of product [72], QM calculations [73], and no reported evidence of high valence iron species in RO-O enzymes through spectroscopic methods in the literature.

Rieske outcomes: Structural differences affecting product formation

The metabolism of aromatic hydrocarbons is arguably the most studied aspect of ROs. These enzymes are well known for their ability to oxidize a wide variety of substrates. NDO-$O_{9816\text{-}4}$ has also been shown to catalyze monooxygenation, sulfoxidation, O- and N-dealkylation, and desaturation along with dioxygenation [63]. Many studies have investigated the ability of ROs to metabolize specific compounds. These studies have created a catalog of substrates for ROs, with product selectivities and specific yields for individual regio- and stereo-isomers [63,74,75]. Overall, these studies have demonstrated the general versatility of ROs with respect to a large number of substrates, and at the same time, demonstrated specificity in product formation for individual substrates. This information, along with structural information, leads to the hypothesis that while the active sites of ROs are amenable to a wide variety of substrates, the orientation of the substrate in a preferred manner determines the product.

Crystal structures of ROs show oxygen and substrate bind in a similar manner regardless of the specific enzyme, with the atom(s) closest to the Fe–O_2 complex being oxidized. Even in the case of OMO-O_{86}, which performs a monohydroxylation on 2-oxoquinoline, this holds true [38]. Interactions between the substrate and active site residues are believed to control the orientation of substrate in the active site.

Table 3
Structurally analogous active site residues for various RO-O enzymes

NDO-$O_{9816\text{-}4}$	NBDO-O_{JS765}	BPDO-O_{B1}	CDO-O_{IP01}	BPDO-O_{RHA1}	NDO-O_{12038}	OMO-O_{86}	CARDO-O_{CA10}
Asn201	Asn199	Asn200	Gln227	Gln217	Asn209	Asn215	Asn177
Phe202	Phe200	Phe201	Phe228	Phe218	Phe210	Leu 302, Gly216	Leu 270, Gly178
Val203	Val201	Ile202	Cys229	Cys219	Val211	Phe217	Phe179
Gly204	Gly202	Gly203	Ser230	Ser220	Gly212	—	—
Asp205	Asp203	Asp204	Asp231	Asp221	Asp213	Asp218	Asp180
Ala206	Gly204	Gly205	Met232	Met222	Ala214	Asn219	Pro181
His208	His206	His207	His234	His224	His216	His221	His183
Val209	Val207	Val208	Ala235	Ala225	Thr217	Ile222	Ile184
His213	His211	His212	His240	His230	His221	His225	His187
Leu217	Leu215	Leu216	Val244	Ile234	Val225	Leu238	Leu200
Phe224	Phe222	Leu223	Leu284	Leu274	Phe293	Val304	Ala259
Leu227	Ile225	Leu226	Leu259	Pro250	Phe236	Pro239	Pro201
Gly251	Gly249	Gly251	Gly276	Gly266	Gly252	Thr294	Ile262
Leu253	Phe251	Ile253	Phe278	Tyr268	Ile254	Tyr292	Ala259
Val260	Asn258	Leu260	Ile288	Ile278	Met309	Trp307	Phe275
His295	Phe293	His293	Ala321	Ala311	Phe293	Val304	Val272
Asn297	Asn295	Asn295	His323	His313	His295	Thr294	Leu270
Leu307	Leu305	Leu305	Leu333	Leu323	Phe307	Gln314	Glu282
Ser310	Ser308	Thr308	Ile336	Ile326	Phe320	Trp307	—
Phe352	Ile350	Phe350	Phe378	Phe368	Phe362	Asn362	Asn330
Trp358	Trp356	Leu356	Tyr384	Phe374	Phe368	Phe361	Phe329

Residues involved in the coordination of the Rieske cluster and mononuclear iron, along with the aspartic acid that bridges the two, are completely conserved in all of the structures of ROs determined to date. These residues have not been shown to alter regio-selectivity, but have been demonstrated to be critical for the function of the enzyme [76,77]. Carredano et al. [29] identified 17 residue side chains that contribute to the overall topology of the NDO-O_{9816-4} active site (Table 3). Mutational studies have demonstrated that alteration of some of these residues can affect the regio-selectivity of product formation in NDO-O_{9816-4} [77–80]. Altered regio-selectivity of product formation after mutation of residues homologous to active site residues in other ROs has also been reported [81–84]. Structures of NDO-O_{9816-4} mutants in complex with naphthalene and phenanthrene show the substrate oriented differently than in wild-type NDO-O_{9816-4} (Ferraro, unpublished). The orientation of the substrate agrees with regio-selectivity of product formation previously determined for these enzymes [77,79,80].

Biotransformation studies have demonstrated a difference in the oxidation of nitroaromatic substrates between NDO-O_{9816-4} and NBDO-O_{JS765}. NDO-O_{9816-4} performs a monooxygenation reaction on nitrotoluenes, hydroxylating the benzylic carbon, while NBDO-O_{JS765} performs a dihydroxylation reaction on the ring [85,86]. Only five active site residues differ between NDO-O_{9816-4} and NBDO-O_{JS765}, and their overall structures are very similar (Fig. 6). The structure of NBDO-O_{JS765} in complex with nitrobenzene shows the substrate oxygens of the nitro group hydrogen bonding with the side chain of Asn258 [36]. This interaction orients the substrate so that the ring is closest to the iron. In NDO-O_{9816-4}, the analogous residue is a valine (V260), which cannot participate in a hydrogen bond. The mutation N258V in NBDO-O_{JS765} changes the regio-selectivity of product formation for 2-nitrotoluene, forming mostly nitrobenzyl alcohol, the product formed by NDO-O_{9816-4}, rather than the catechol (R. Parales, personal communication). A similar mutation in 2-nitrotoluene dioxygenase, N258V, also eliminates the formation of the catechol from 2-nitrotoluene, producing only the nitrobenzyl alcohol [84]. This suggests that the nitrotoluenes are tethered in place by Asn258 at the active site, helping to control the regio-selectivity of product formation.

In NDO-O_{9816-4} and NDO-O_{12038}, there is a similar anchoring of the nitrogen atom of indole to a hydrogen bond with the main chain oxygen of the bridging aspartic acid [29]. In NDO-O_{9816-4}, the substrate is not directly above the mononuclear iron, allowing the substrate to approach with two carbons equidistant from the iron (Fig. 6). NDO-O_{12038} shares only a 30% sequence identity with NDO-O_{9816-4}, but is expressed in the presence of naphthalene as a growth substrate [87] and like NDO-O_{9816-4} converts it to naphthalene-*cis*-dihydrodiol [44]. The overall structures of these two enzymes are very similar with a RMSD of 1.58 Å over 359 C_α atoms of the α-subunit. Most of the active site variability between the two enzymes is in the residues near the distal ring binding site of the substrate [35]. However, structures of indole-bound forms of NDO-O_{9816-4} and NDO-O_{12038} show that the substrate binds in the same place next to the iron. Moreover, like NDO-O_{9816-4}, there is no change in the active site of NDO-O_{12038} upon indole binding.

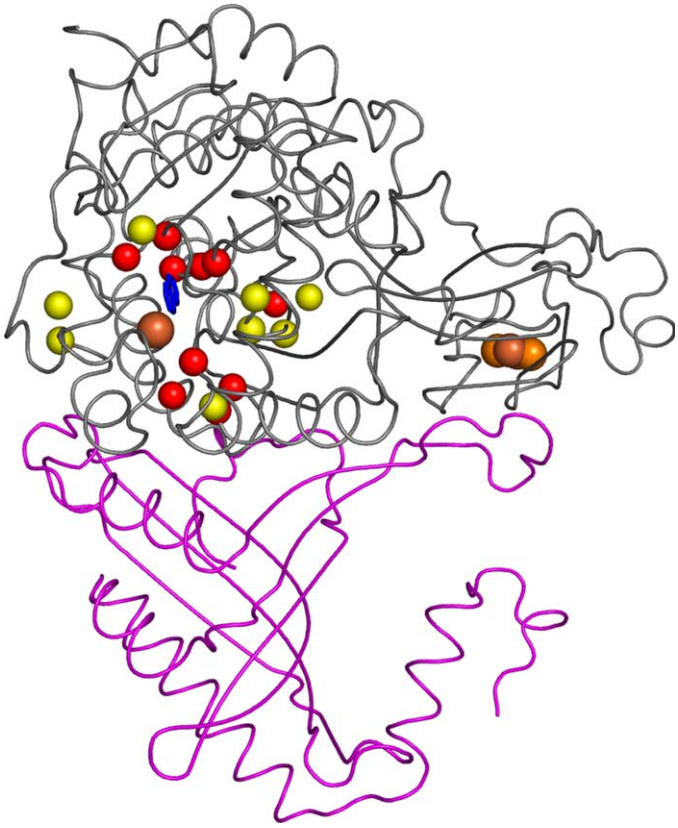

Fig. 6. A cartoon representation of a single NDO-O_{9816-4} α (grey)–β (magenta) dimer. The Rieske cluster and mononuclear irons are shown in orange. Naphthalene bound to the active site in NDO-O_{9816-4} is blue. Shown in red spheres are residues that have been shown to affect the regio-selectivity of product formation in NDO-O_{9816-4}. Yellow spheres show the residues that comprise regions I–IV in BPDO-O enzymes. These residues have been shown to strongly correlate with the ability of BPDO-O enzymes to metabolize either *ortho–meta* substituted or *para* substituted PCBs. This structural representation suggests that the residues responsible for substrate selectivity for BPDOs are in the same region, the mononuclear active site, as the residues responsible for regio-selectivity of product formation in NDO-O_{9816-4}, suggesting that these both work through a similar structural mechanism.

The crystal structure of OMO-O_{86} provides another example of substrate tethering [38]. A hydrogen bond exists between the substrate 2-oxoquinoline and the main chain oxygen of Gly216, orienting the substrate in the active site. The active site of OMO-O_{86} allows space for the substrate to bind almost directly above the mononuclear iron, allowing for carbon 8 of the substrate to orient closest to the mononuclear iron. The tethering of substrate by a single hydrogen bond to control orientation is a repeated scheme in these enzymes and suggests one way these enzymes control regio-selectivity of product formation.

Rieske choices: Structural differences affecting substrate specificity

In contrast to naphthalene dioxygenase, substrate specificity rather than product formation has been extensively studied in biphenyl dioxygenase systems, due to their ability to oxidize polychlorinated biphenyls (PCBs). Many biphenyl metabolizing Rieske dioxygenases have been isolated from PCB-degrading strains of bacteria such as *B. xenovorans* LB400 [88], *Pseudomonas pseudoalcaligenes* KF707 [89], and *Rhodococcus* sp. strain RHA1[90] and subsequently characterized. These enzymes have been classified into two groups based upon the types of PCBs they are able to metabolize. LB400 type BPDOs are able to oxidize *ortho–meta* substituted congeners, such as 2,5,2′5′-tetrachlorobiphenyl, and KF707 type BPDOs are able to oxidize double *para*-substituted congeners, such as 4,4′-dicholorobiphenyl [91].

Furusawa et al. [34] determined the structure of BPDO-O_{RHA1} from *Rhodococcus* sp. strain RHA1 to 2.2 Å and the structure of the enzyme-biphenyl complex to 2.6 Å. They observed a conformational change in the active site upon substrate binding, something not seen in previous structures of NDO-$O_{9816\text{-}4}$. It was also observed that the binding pocket in the substrate-free active site was too small to accommodate biphenyl, but conformational changes upon binding the substrate enlarged the binding pocket. These conformational changes occurred closer to the entrance of the active site, where the distal ring of biphenyl bound. Active site residues nearest the mononuclear iron did not exhibit a significant shift. A similar pattern of flexibility has been observed in structures of OMO-O_{86} substrate-bound and substrate-free enzyme [38]. Loop regions at the entrance to the active site in crystal structures of other RO-O enzymes are disordered or have high temperature factors. This flexibility may help allow the accommodation of different substrates of various sizes and shapes.

The atomic structure of CDO-O_{IP01} determined by Dong et al. [37] was solved to 2.2 Å resolution. In their analysis, they compare the structure of CDO-O_{IP01} to NDO-$O_{9816\text{-}4}$ and BPDO-O_{RHA1}, as well as dock the small molecule into the active site of CDO-O_{IP01}. A study of PCB-degrading bacteria identified regions in biphenyl dioxygenases that had high sequence correlation with the phenotype of broad or narrow substrate specificity [92]. Sequence alignments and subsequent structural positioning demonstrated that regions II–IV were involved in the formation of the active site. Mutations in regions III and IV were also found to have large effects on substrate specificity, which fits with structural modeling. The sequences of CDO-O_{IP01} and BPDO-O_{RHA1} more closely resemble that of broad specificity PCB-degrading enzymes, such as biphenyl dioxygenase from LB400, while NDO-$O_{9816\text{-}4}$ more closely resembles that of narrow specificity. Biphenyl docked in the active site of CDO-O_{IP01} was shown to have interactions with side chains of residues in regions II and III. Region I was determined to be the loop region that forms a bend between the histidines that coordinate the mononuclear iron. There is significant deviation between the structure of CDO-O_{IP01}, BPDO-O_{RHA1}, and NDO-$O_{9816\text{-}4}$ in region I. The most notable difference is that this region is one residue shorter in NDO-$O_{9816\text{-}4}$ as compared to the other two dioxygenases. This creates a bent helix in NDO-$O_{9816\text{-}4}$ in this region, while a bulge is present in the other two structures. Clearly, this region is located in a critical area for enzymatic function, as it is involved in iron coordination; however, it is not clear how mutations in this area may affect substrate specificity.

The preliminary structure of biphenyl dioxygenase from *S. yanoikuyae* strain B1 [93,94] (gene B1bphA1fA2f) has recently been determined to 1.75 Å (Ferraro, unpublished work). BPDO-O_{B1} originates from a bacterium shown to oxidize 4 or 5 ring aromatic hydrocarbons, such as chrysene and benzo[*a*]pyrene [95]. Multiple Rieske oxygenase genes exist in this organism and substrate profiles for individual dioxygenases have not been determined. Structural analysis of BPDO-O_{B1} using the software package Voidoo [96] shows a large active site, ~41 $Å^3$, compared to BPDO-O_{RHA1}, ~27$Å^3$. The active site of BPDO-O_{B1} enlarges to ~55 $Å^3$ upon binding of biphenyl. The size and shape of the active site suggests that this enzyme would be able to accommodate 4 or 5 ring substrates. Currently, biochemical studies are being performed to determine if this enzyme is responsible for the oxidation of large arenes by *S. yanoikuyae* B1.

Many studies have investigated the effects of mutations on the substrate specificity of ROs, especially with respect to the BPDO-O enzymes [97]. Overall, mutations shown to affect regio- and stereo-selectivity of product formation in NDO-$O_{9816\text{-}4}$ and mutations shown to alter substrate specificity in BPDO-O enzymes lie in relatively similar regions (Fig. 7). These regions tend to form the topology of the active site, influencing access and orientation of substrate. With regard to main-chain structure, the active sites tend to be structurally similar near the mononuclear iron and diverge toward the entrance of the active site. Studies of hybrid ROs have also demonstrated altered regio-selectivity of product formation and substrate specificity [42,98–100]. While there is no structural work demonstrating the differences in these enzymes compared to the wild-type enzymes from which they derive, it is believed that changes are likely due to alteration of active site topology. These alterations may be simple and directly change the active site topology through side chain residues; however, others may be more complex, indirectly altering the general topology of the active site.

Rieske ventures: Applications and rational engineering

Because of their versatility, these enzymes have been targeted as platforms for large-scale biosynthesis of aromatic compounds. One of the most well-known applications for ROs is the biosynthesis of indigo, a small aromatic dye used in commercial applications. Produced from indole

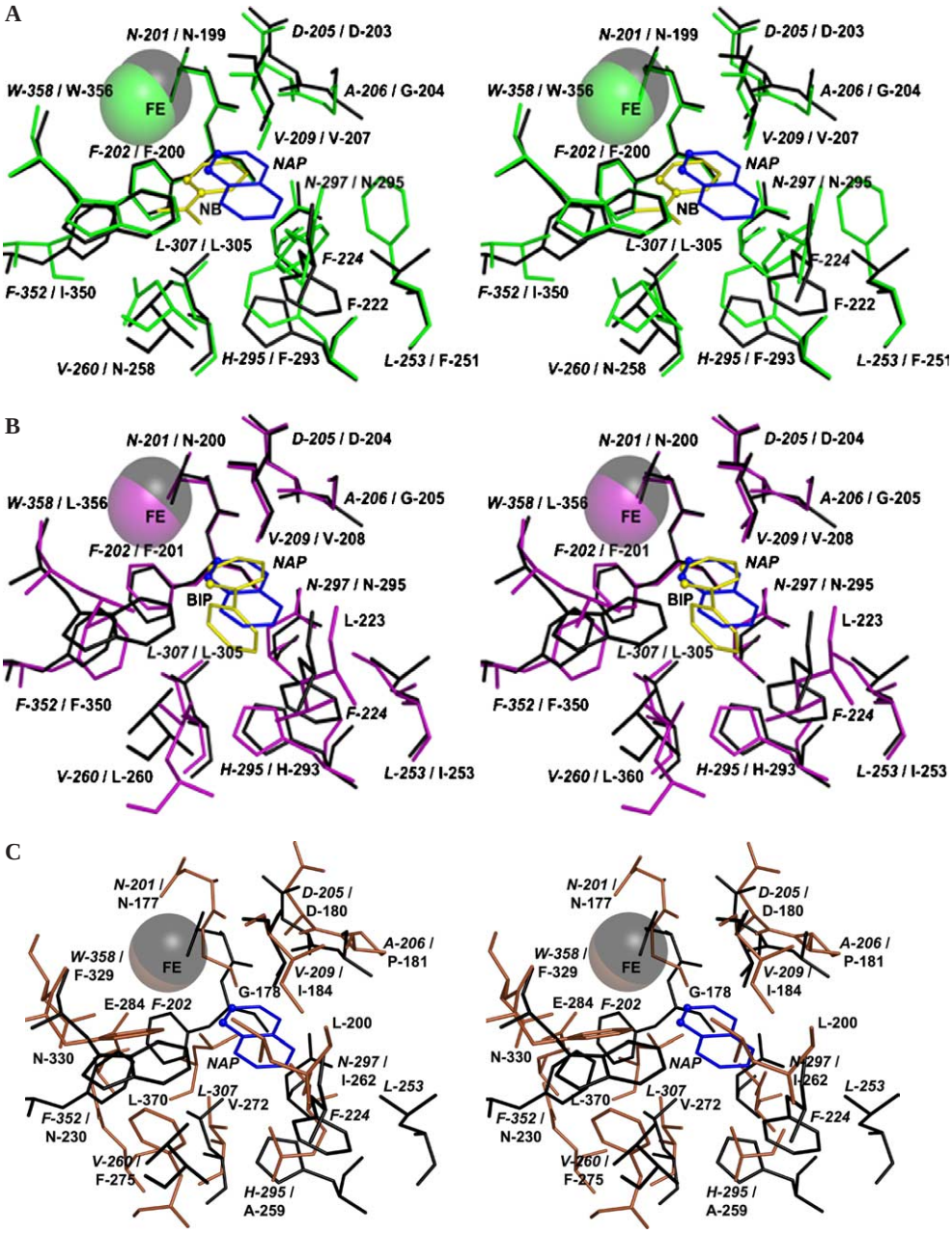

Fig. 7. Overlay of RO-O active sites and product (if available) with the active site of NDO-$O_{9816\text{-}4}$ and naphthalene. The structural overlays are as follows: (A) NBDO-O_{JS765} with nitrobenzene, (B) BPDO-O_{B1} with biphenyl, (C) CARDO-O_{CA10}, (D) CDO-O_{IP01}, (E) BPDO-O_{RHA1} with biphenyl, (F) NDO-O_{12038} and indole, and (G) OMO-O_{86} with 2-oxoquinoline. Spheres are shown on the substrates carbons (where available) that are oxidized by the enzyme. These overlays demonstrate the overall conserved structure of the active site between RO-O enzymes; however, some differences are present and many have been suggested to play a role in the differences in substrate specificity and regio-selection of product formation between the enzymes. The color scheme for the RO-O enzymes is the same as in Fig. 4. Images were made with PyMOL [106].

by naphthalene dioxygenase, *cis*-indole-2,3-dihydrodiol was shown to spontaneously dehydrate to form indigo [101]. Other applications for *cis*-dihydrodiols formed by ROs have also been demonstrated, such as the generation of chiral precursors for the synthesis of drugs such as indinavir sulfate [102–104]. These enzyme systems have also shown promise as platforms for bioremediation on the basis of the 200+ arene substrates these enzymes can act upon [74]. Biodegradation of polyaromatic hydrocarbons, with an emphasis on polychlorinated biphenyls, has been investigated extensively with the biphenyl dioxygenases. Directed evolution studies have been used to improve enzyme activity toward target compounds [97,105]. Structural information has helped explain some of the trends found in directed evolution studies and narrow the number of residues in mutation studies to the most likely to effect enzyme function. We hope in the future this information will allow for rational design of specific activity into ROs.

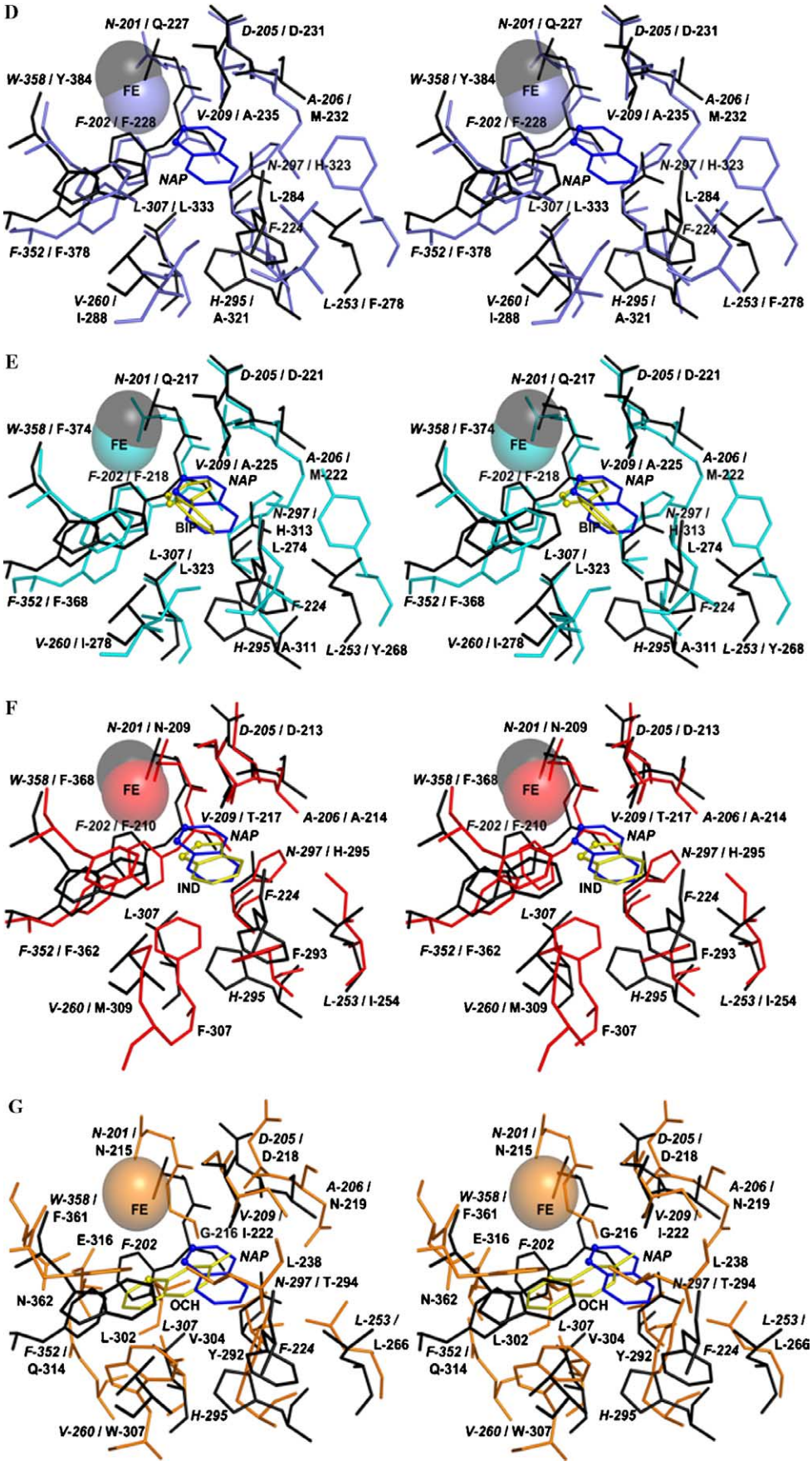

Fig. 7. (*continued*).

In both biosynthesis and bioremediation applications, structural information has helped explain how ROs function. Clues as to how researchers can manipulate these proteins to perform novel reactions and improve efficacy can be extracted from structural information. The presence of this class of enzymes in a number of different organisms and large sequence variation (albeit conserved structural features) suggests that these enzymes are versatile catalysts and have been used in nature extensively for degradation of a variety of compounds [74]. The studies of the relationships between these enzymes' structure and function have revealed several of nature's secrets. They have given insight into how enzymes manage to have rather promiscuous substrate specificity, while maintaining stereo- and regio-selectivity of product formation. In addition, these studies have helped us understand how nature has devised ways to control electrons, create and utilize reactive oxygen specie and activate carbon–carbon bonds, chemistry crucial for life on earth.

Acknowledgments

We wish to acknowledge the great support we have had for this work from Prof. David Gibson, Prof. Hans Eklund and Dr. Rebecca Parales. We would like to thank Adam Okerlund, Eric Brown, Jonathan Mowers, Wendie Dockstader, Nathan Coussens, Debra Ferraro, Heather Hansen and Rosmarie Friemann for critical reading and suggestions for the manuscript. S.R. would like to acknowledge Bjorn Kauppi, Enrique Carredano, Juan Parales and Devapriya Choudhoury for being great collaborators. We also would like to thank Hideaki Nojiri, Eric Brown, Chi-Li Yu, Andreas Karlsson and Kyoung Lee for access to unpublished data during the writing of this review. D.F. and L.G. are recipients of University of Iowa Center for Biocatalysis and Bioprocessing fellowships and D.F. is also supported through a Medical Scientist Trainee Program traineeship at UI. S.R. acknowledges financial support from USPHS Grant # GM62904 and a grant from NSF-ERC Grant # EEC-031068.

References

[1] B.C. Axcell, P.J. Geary, Purification and some properties of a soluble benzene-oxidizing system from a strain of *Pseudomonas*, Biochem. J. 146 (1975) 173–183.
[2] D.T. Gibson, J.R. Koch, R.E. Kallio, Oxidative degradation of aromatic hydrocarbons by microorganisms. I. Enzymatic formation of catechol from benzene, Biochemistry 7 (1968) 2653–2662.
[3] D.T. Gibson, G.E. Cardini, F.C. Maseles, R.E. Kallio, Incorporation of oxygen-18 into benzene by *Pseudomonas putida*, Biochemistry 9 (1970) 1631–1635.
[4] D.M. Jerina, J.W. Daly, A.M. Jeffrey, D.T. Gibson, *Cis*-1,2-dihydroxy-1a a bacterial metabolite from naphthalene, Arch. Biochem. Biophys. 142 (1971) 394–396.
[5] A.M. Jeffrey, H.J. Yeh, D.M. Jerina, T.R. Patel, J.F. Davey, D.T. Gibson, Initial reactions in the oxidation of naphthalene by *Pseudomonas putida*, Biochemistry 14 (1975) 575–584.
[6] D.T. Gibson, M. Hensley, H. Yoshioka, T.J. Mabry, Formation of (+)-*cis*-2,3-dihydroxy-1-methylcyclohexa-4,6-diene from toluene by *Pseudomonas putida*, Biochemistry 9 (1970) 1626–1630.
[7] H. Ziffer, D.M. Jerina, D.T. Gibson, V.M. Kobal, Absolute stereochemistry of the (+)-*cis*-1,2-dihydroxy-3-methylcyclohexa-3,5-diene produced from toluene by *Pseudomonas putida*, J. Am. Chem. Soc. 95 (1973) 4048–4049.
[8] R. Cammack, E. Gay, J.K. Shergill, Studies of hyperfine interactions in [2Fe–2S] proteins by EPR and double resonance spectroscopy, Coordin. Chem. Rev. 192 (1999) 1003–1022.
[9] J.S. Rieske, Studies on the electron transfer system—properties of a new oxidation–reduction component of the respiratory chain as studied by electron paramagnetic resonance spectroscopy, J. Biol. Chem. 239 (1968) 3017–3022.
[10] J.S. Rieske, D.H. MacLennan, R. Coleman, Isolation and properties of an iron–protein from the (reduced coenzyme Q)-cytochrome *c* reductase complex of the respiratory chain, Biochem. Biophys. Res. Commun. 15 (1964) 338–344.
[11] B. Kauppi, K. Lee, E. Carredano, R.E. Parales, D.T. Gibson, H. Eklund, S. Ramaswamy, Structure of an aromatic-ring-hydroxylating dioxygenase-naphthalene 1,2-dioxygenase, Structure 6 (1998) 571–586.
[12] J.F. Cline, B.M. Hoffman, W.B. Mims, E. LaHaie, D.P. Ballou, J.A. Fee, Evidence for N coordination to Fe in the [2Fe–2S] clusters of Thermus Rieske protein and phthalate dioxygenase from *Pseudomonas*, J. Biol. Chem. 260 (1985) 3251–3254.
[13] J.A. Fee, K.L. Findling, T. Yoshida, R. Hille, G.E. Tarr, D.O. Hearshen, W.R. Dunham, E.P. Day, T.A. Kent, E. Munck, Purification and characterization of the Rieske iron–sulfur protein from *Thermus thermophilus*. Evidence for a [2Fe–2S] cluster having non-cysteine ligands, J. Biol. Chem. 259 (1984) 124–133.
[14] D. Kuila, J.A. Fee, Evidence for a redox-linked ionizable group associated with the [2Fe–2S] cluster of Thermus Rieske protein, J. Biol. Chem. 261 (1986) 2768–2771.
[15] Y. Zu, M.M. Couture, D.R. Kolling, A.R. Crofts, L.D. Eltis, J.A. Fee, J. Hirst, Reduction potentials of Rieske clusters: importance of the coupling between oxidation state and histidine protonation state, Biochemistry 42 (2003) 12400–12408.
[16] N.J. Cosper, D.M. Eby, A. Kounosu, N. Kurosawa, E.L. Neidle, D.M. Kurtz Jr., T. Iwasaki, R.A. Scott, Redox-dependent structural changes in archaeal and bacterial Rieske-type [2Fe–2S] clusters, Protein Sci. 11 (2002) 2969–2973.
[17] E. Denke, T. Merbitz-Zahradnik, O.M. Hatzfeld, C.H. Snyder, T.A. Link, B.L. Trumpower, Alteration of the midpoint potential and catalytic activity of the Rieske iron–sulfur protein by changes of amino acids forming hydrogen bonds to the iron–sulfur cluster, J. Biol. Chem. 273 (1998) 9085–9093.
[18] M. Guergova-Kuras, R. Kuras, N. Ugulava, I. Hadad, A.R. Crofts, Specific mutagenesis of the rieske iron–sulfur protein in *Rhodobacter sphaeroides* shows that both the thermodynamic gradient and the pK of the oxidized form determine the rate of quinol oxidation by the bc(1) complex, Biochemistry 39 (2000) 7436–7444.
[19] T. Schroter, O.M. Hatzfeld, S. Gemeinhardt, M. Korn, T. Friedrich, B. Ludwig, T.A. Link, Mutational analysis of residues forming hydrogen bonds in the Rieske [2Fe–2S] cluster of the cytochrome bc1 complex in *Paracoccus denitrificans*, Eur. J. Biochem. 255 (1998) 100–106.
[20] C.L. Colbert, M.M. Couture, L.D. Eltis, J.T. Bolin, A cluster exposed: structure of the Rieske ferredoxin from biphenyl dioxygenase and the redox properties of Rieske Fe–S proteins, Struct. Fold Des. 8 (2000) 1267–1278.
[21] C.C. Correll, C.J. Batie, D.P. Ballou, M.L. Ludwig, Phthalate dioxygenase reductase: a modular structure for electron transfer from pyridine nucleotides to [2Fe–2S], Science 258 (1992) 1604–1610.
[22] A. Karlsson, Z.M. Beharry, D. Matthew Eby, E.D. Coulter, E.L. Neidle, D.M. Kurtz Jr., H. Eklund, S. Ramaswamy, X-ray crystal structure of benzoate 1,2-dioxygenase reductase from *Acinetobacter* sp. strain ADP1, J. Mol. Biol. 318 (2002) 261–272.
[23] T. Senda, T. Yamada, N. Sakurai, M. Kubota, T. Nishizaki, E. Masai, M. Fukuda, Y. Mitsuidagger, Crystal structure of NADH-

dependent ferredoxin reductase component in biphenyl dioxygenase, J. Mol. Biol. 304 (2000) 397–410.
[24] K. Lee, R. Friemann, J.V. Parales, D.T. Gibson, S. Ramaswamy, Purification, crystallization and preliminary X-ray diffraction studies of the three components of the toluene 2,3-dioxygenase enzyme system, Acta Crystallogr. F Struct. Bio. Cryst. Commun. 61 (2005); R. Friemann, Molecular Biology, Swedish University of Agricultural Sciences, Uppsala, Sweden, 2005.
[25] M.M. Couture, C.L. Colbert, E. Babini, F.I. Rosell, A.G. Mauk, J.T. Bolin, L.D. Eltis, Characterization of BphF, a Rieske-type ferredoxin with a low reduction potential, Biochemistry 40 (2001) 84–92.
[26] A. Karlsson, in: Molecular Biology, Swedish University of Agricultural Sciences, Uppsala, Sweden, 2002.
[27] J.W. Nam, H. Noguchi, Z. Fujimoto, H. Mizuno, Y. Ashikawa, M. Abo, S. Fushinobu, N. Kobashi, T. Wakagi, K. Iwata, T. Yoshida, H. Habe, H. Yamane, T. Omori, H. Nojiri, Crystal structure of the ferredoxin component of carbazole 1,9a-dioxygenase of *Pseudomonas resinovorans* strain CA10, a novel Rieske non-heme iron oxygenase system, Proteins 58 (2005) 779–789.
[28] A.G. Murzin, S.E. Brenner, T. Hubbard, C. Chothia, SCOP: a structural classification of proteins database for the investigation of sequences and structures, J. Mol. Biol. 247 (1995) 536–540.
[29] E. Carredano, A. Karlsson, B. Kauppi, D. Choudhury, R.E. Parales, J.V. Parales, K. Lee, D.T. Gibson, H. Eklund, S. Ramaswamy, Substrate binding site of naphthalene 1,2-dioxygenase: functional implications of indole binding, J. Mol. Biol. 296 (2000) 701–712.
[30] E. Carredano, B. Kauppi, D. Choudhury, R.E. Parales, K. Lee, D.T. Gibson, H. Eklund, S. Ramaswamy, Implications for substrate specificity of naphthalene 1,2-dioxygenase from the refined crystal structure 451, J. Inorg. Biochem. 74 (1999) 21.
[31] E. Carredano, B. Kauppi, D. Choudhury, S. Ramaswamy, Pseudosymmetry characterization and refinement of a trigonal crystal form of naphthalene 1,2-dioxygenase, Acta Crystallogr. D. Biol. Crystallogr. 56 (Pt. 3) (2000) 313–321.
[32] A. Karlsson, J.V. Parales, R.E. Parales, D.T. Gibson, H. Eklund, S. Ramaswamy, Crystal structure of naphthalene dioxygenase: side-on binding of dioxygen to iron, Science 299 (2003) 1039–1042.
[33] A. Karlsson, J.V. Parales, R.E. Parales, D.T. Gibson, H. Eklund, S. Ramaswamy, NO binding to naphthalene dioxygenase, J. Biol. Inorg. Chem. (2005).
[34] Y. Furusawa, V. Nagarajan, M. Tanokura, E. Masai, M. Fukuda, T. Senda, Crystal structure of the terminal oxygenase component of biphenyl dioxygenase derived from *Rhodococcus* sp. strain RHA1, J. Mol. Biol. 342 (2004) 1041–1052.
[35] L. Gakhar, Z.A. Malik, C.C. Allen, D.A. Lipscomb, M.J. Larkin, S. Ramaswamy, Structure and increased thermostability of Rhodococcus sp. naphthalene 1,2-dioxygenase, J. Bacteriol. (2005) in press.
[36] R. Friemann, M.M. Ivkovic-Jensen, D.J. Lessner, C.L. Yu, D.T. Gibson, R.E. Parales, H. Eklund, S. Ramaswamy, Structural insight into the dioxygenation of nitroarene compounds: the crystal structure of nitrobenzene dioxygenase, J. Mol. Biol. 348 (2005) 1139–1151.
[37] X. Dong, S. Fushinobu, E. Fukuda, T. Terada, S. Nakamura, K. Shimizu, H. Nojiri, T. Omori, H. Shoun, T. Wakagi, Crystal structure of the terminal oxygenase component of cumene dioxygenase from *Pseudomonas fluorescens* IP01, J. Bacteriol. 187 (2005) 2483–2490.
[38] B.M. Martins, T. Svetlitchnaia, H. Dobbek, 2-Oxoquinoline 8-monooxygenase oxygenase component: active site modulation by Rieske-[2Fe–2S] center oxidation/reduction, Structure 13 (2005) 817–824.
[39] H. Nojiri, Y. Ashikawa, H. Noguchi, J.W. Nam, M. Urata, Z. Fujimoto, H. Uchimura, T. Terada, S. Nakamura, K. Shimizu, T. Yoshida, H. Habe, T. Omori, Structure of the terminal oxygenase component of angular dioxygenase, carbazole 1,9a-dioxygenase, J. Mol. Biol. (2005).
[40] T. Lundqvist, J. Rice, C.N. Hodge, G.S. Basarab, J. Pierce, Y. Lindqvist, Crystal structure of scytalone dehydratase—a disease determinant of the rice pathogen, *Magnaporthe grisea*, Structure 2 (1994) 937–944.
[41] T.L. Bullock, W.D. Clarkson, H.M. Kent, M. Stewart, The 1.6 angstroms resolution crystal structure of nuclear transport factor 2 (NTF2), J. Mol. Biol. 260 (1996) 422–431.
[42] Y. Hurtubise, D. Barriault, M. Sylvestre, Involvement of the terminal oxygenase beta subunit in the biphenyl dioxygenase reactivity pattern toward chlorobiphenyls, J. Bacteriol. 180 (1998) 5828–5835.
[43] B.D. Ensley, D.T. Gibson, Naphthalene dioxygenase: purification and properties of a terminal oxygenase component, J. Bacteriol. 155 (1983) 505–511.
[44] M.J. Larkin, C.C. Allen, L.A. Kulakov, D.A. Lipscomb, Purification and characterization of a novel naphthalene dioxygenase from *Rhodococcus* sp. strain NCIMB12038, J. Bacteriol. 181 (1999) 6200–6204.
[45] C. Batie, D. Ballou, C. Corell, Phthalate dioxygenase reductase and related flavin–iron–sulfur containing electron transferases, in: F. Muller (Ed.), Chemistry and Biochemistry of Flavoenzymes, CRC Press, Boca Raton, FL, 1992, pp. 542–556.
[46] G.T. Gassner, Structure and mechanism of the iron–sulfur flavoprotein phthalate dioxygenase reductase, FASEB J. 9 (1995) 1411–1418.
[47] C. Werlen, H.P. Kohler, J.R. van der Meer, The broad substrate chlorobenzene dioxygenase and *cis*-chlorobenzene dihydrodiol dehydrogenase of *Pseudomonas* sp. strain P51 are linked evolutionarily to the enzymes for benzene and toluene degradation, J. Biol. Chem. 271 (1996) 4009–4016.
[48] D.T. Gibson, R.E. Parales, Aromatic hydrocarbon dioxygenases in environmental biotechnology, Curr. Opin. Biotechnol. 11 (2000) 236–243.
[49] J.W. Nam, H. Nojiri, T. Yoshida, H. Habe, H. Yamane, T. Omori, New classification system for oxygenase components involved in ring-hydroxylating oxygenations, Biosci. Biotechnol. Biochem. 65 (2001) 254–263.
[50] A. Bassan, T. Borowski, P.E. Siegbahn, Quantum chemical studies of dioxygen activation by mononuclear non-heme iron enzymes with the 2-His-1-carboxylate facial triad, Dalton Trans. (2004) 3153–3162.
[51] M. Costas, M.P. Mehn, M.P. Jensen, L. Que Jr., Dioxygen activation at mononuclear nonheme iron active sites: enzymes, models, and intermediates, Chem. Rev. 104 (2004) 939–986.
[52] S.J. Lange, L. Que, Oxygen activating nonheme iron enzymes, Curr. Opin. Chem. Bio. 2 (1998) 159–172.
[53] L. Que Jr., One motif—many different reactions, Nat. Struct. Biol. 7 (2000) 182–184.
[54] L.P. Wackett, Mechanism and applications of Rieske non-heme iron dioxygenases, Enzyme Microb. Technol. 31 (2002) 577–587.
[55] E.I. Solomon, T.C. Brunold, M.I. Davis, J.N. Kemsley, S.K. Lee, N. Lehnert, F. Neese, A.J. Skulan, Y.S. Yang, J. Zhou, Geometric and electronic structure/function correlations in non-heme iron enzymes, Chem. Rev. 100 (2000) 235–350.
[56] L. Que Jr., R.Y. Ho, Dioxygen activation by enzymes with mononuclear non-heme iron active sites, Chem. Rev. 96 (1996) 2607–2624.
[57] M.D. Wolfe, J.V. Parales, D.T. Gibson, J.D. Lipscomb, Single turnover chemistry and regulation of O2 activation by the oxygenase component of naphthalene 1,2-dioxygenase, J. Biol. Chem. 276 (2001) 1945–1953.
[58] M.D. Wolfe, D.J. Altier, A. Stubna, C.V. Popescu, E. Munck, J.D. Lipscomb, Benzoate 1,2-dioxygenase from *Pseudomonas putida*: single turnover kinetics and regulation of a two-component Rieske dioxygenase, Biochemistry 41 (2002) 9611–9626.
[59] H.T. Tsang, C.J. Batie, D.P. Ballou, J.E. Penner-Hahn, X-ray absorption spectroscopy of the [2Fe–2S] Rieske cluster in *Pseudomonas cepacia* phthalate dioxygenase. Determination of core dimensions and iron ligation, Biochemistry 28 (1989) 7233–7240.
[60] R.E. Parales, J.V. Parales, D.T. Gibson, Aspartate 205 in the catalytic domain of naphthalene dioxygenase is essential for activity, J. Bacteriol. 181 (1999) 1831–1837.

[61] Z.M. Beharry, D.M. Eby, E.D. Coulter, R. Viswanathan, E.L. Neidle, R.S. Phillips, D.M. Kurtz Jr., Histidine ligand protonation and redox potential in the Rieske dioxygenases: role of a conserved aspartate in anthranilate 1,2-dioxygenase, Biochemistry 42 (2003) 13625–13636.
[62] E.L. Hegg, L. Que Jr., The 2-His-1-carboxylate facial triad—an emerging structural motif in mononuclear non-heme iron(II) enzymes, Eur. J. Biochem. 250 (1997) 625–629.
[63] S.M. Resnick, K. Lee, D.T. Gibson, Diverse reactions catalyzed by naphthalene dioxygenase from *Pseudomonas* sp. strain NCIB 9816, J. Ind. Microbiol. Biotechnol. 17 (1996) 438–457.
[64] T.C. Yang, M.D. Wolfe, M.B. Neibergall, Y. Mekmouche, J.D. Lipscomb, B.M. Hoffman, Modulation of substrate binding to naphthalene 1,2-dioxygenase by Rieske cluster reduction/oxidation, J. Am. Chem. Soc. 125 (2003) 2034–2035.
[65] T.C. Yang, M.D. Wolfe, M.B. Neibergall, Y. Mekmouche, J.D. Lipscomb, B.M. Hoffman, Substrate binding to NO-ferro-naphthalene 1,2-dioxygenase studied by high-resolution Q-band pulsed 2H-ENDOR spectroscopy, J. Am. Chem. Soc. 125 (2003) 7056–7066.
[66] M.D. Wolfe, J. Parales, K. Lee, D.T. Gibson, J.D. Lipscomb, Substrate binding to the mononuclear ferrous ion of the Rieske dioxygenase naphthalene 1,2-dioxygenase from *Pseudomonas* sp. NCIB 9816-4, J. Inorg. Biochem. 74 (1999) 339.
[67] F.H. Bernhardt, H.U. Meisch, Reactivation studies on putidamonooxin—the monooxygenase of a 4-methoxybenzoate *O*-demethylase from *Pseudomonas putida*, Biochem. Biophys. Res. Commun. 93 (1980) 1247–1253.
[68] W.C. Suen, D.T. Gibson, Isolation and preliminary characterization of the subunits of the terminal component of naphthalene dioxygenase from *Pseudomonas putida* NCIB 9816-4, J. Bacteriol. 175 (1993) 5877–5881.
[69] C.J. Batie, E. LaHaie, D.P. Ballou, Purification and characterization of phthalate oxygenase and phthalate oxygenase reductase from *Pseudomonas cepacia*, J. Biol. Chem. 262 (1987) 1510–1518.
[70] D. Ballou, C. Batie, Phthalate oxygenase, a Rieske iron–sulfur protein from *Pseudomonas cepacia*, Progr. Clin. Biol. Res. 274 (1988) 211–226.
[71] K. Lee, Benzene-induced uncoupling of naphthalene dioxygenase activity and enzyme inactivation by production of hydrogen peroxide, J. Bacteriol. 181 (1999) 2719–2725.
[72] M.D. Wolfe, J.D. Lipscomb, Hydrogen peroxide-coupled *cis*-diol formation catalyzed by naphthalene 1,2-dioxygenase, J. Biol. Chem. 278 (2003) 829–835.
[73] A. Bassan, M.R. Blomberg, P.E. Siegbahn, A theoretical study of the *cis*-dihydroxylation mechanism in naphthalene 1,2-dioxygenase, J. Biol. Inorg. Chem. 9 (2004) 439–452.
[74] T. Hudlicky, D. Gonzalez, D.T. Gibson, Enzymatic dihydroxylation of aromatics in enantioselective synthesis: expanding asymmetric methodology, Aldrichim. Acta 32 (1999) 35–62.
[75] D.R. Boyd, N.D. Sharma, C.C. Allen, Aromatic dioxygenases: molecular biocatalysis and applications, Curr. Opin. Biotechnol. 12 (2001) 564–573.
[76] H. Jiang, R.E. Parales, N.A. Lynch, D.T. Gibson, Site-directed mutagenesis of conserved amino acids in the alpha subunit of toluene dioxygenase: potential mononuclear non-heme iron coordination sites, J. Bacteriol. 178 (1996) 3133–3139.
[77] R.E. Parales, K. Lee, S.M. Resnick, H. Jiang, D.J. Lessner, D.T. Gibson, Substrate specificity of naphthalene dioxygenase: effect of specific amino acids at the active site of the enzyme, J. Bacteriol. 182 (2000) 1641–1649.
[78] R.E. Parales, The role of active-site residues in naphthalene dioxygenase, J. Ind. Microbiol. Biotechnol. 30 (2003) 271–278.
[79] R.E. Parales, S.M. Resnick, C.L. Yu, D.R. Boyd, N.D. Sharma, D.T. Gibson, Regioselectivity and enantioselectivity of naphthalene dioxygenase during arene *cis*-dihydroxylation: control by phenylalanine 352 in the alpha subunit, J. Bacteriol. 182 (2000) 5495–5504.
[80] C.L. Yu, R.E. Parales, D.T. Gibson, Multiple mutations at the active site of naphthalene dioxygenase affect regioselectivity and enantioselectivity, J. Ind. Microbiol. Biotechnol. 27 (2001) 94–103.
[81] B.G. Keenan, T. Leungsakul, B.F. Smets, M.A. Mori, D.E. Henderson, T.K. Wood, Protein engineering of the archetypal nitroarene dioxygenase of *Ralstonia* sp. strain U2 for activity on aminonitrotoluenes and dinitrotoluenes through alpha-subunit residues leucine 225, phenylalanine 350, and glycine 407, J. Bacteriol. 187 (2005) 3302–3310.
[82] K. Pollmann, V. Wray, H.J. Hecht, D.H. Pieper, Rational engineering of the regioselectivity of TecA tetrachlorobenzene dioxygenase for the transformation of chlorinated toluenes, Microbiology 149 (2003) 903–913.
[83] B.G. Keenan, T. Leungsakul, B.F. Smets, T.K. Wood, Saturation mutagenesis of *Burkholderia cepacia* R34 2,4-dinitrotoluene dioxygenase at DntAc valine 350 for synthesizing nitrohydroquinone, methylhydroquinone, and methoxyhydroquinone, Appl. Environ. Microbiol. 70 (2004) 3222–3231.
[84] K.-S. Lee, J.V. Parales, R. Friemann, R.E. Parales, Active site residues controlling substrate specificity in 2-nitrotoluene dioxygenase from *Acidovorax* sp. strain JS42, J. Ind. Microbiol. Biotechnol. (2005) in press.
[85] D.J. Lessner, G.R. Johnson, R.E. Parales, J.C. Spain, D.T. Gibson, Molecular characterization and substrate specificity of nitrobenzene dioxygenase from *Comamonas* sp. strain JS765, Appl. Environ. Microbiol. 68 (2002) 634–641.
[86] W.C. Suen, B.E. Haigler, J.C. Spain, 2,4-Dinitrotoluene dioxygenase from *Burkholderia* sp. strain DNT: similarity to naphthalene dioxygenase, J. Bacteriol. 178 (1996) 4926–4934.
[87] C.C.R. Allen, D.R. Boyd, M.J. Larkin, K.A. Reid, N.D. Sharma, K. Wilson, Metabolism of naphthalene, 1-naphthol, indene, and indole by *Rhodococcus* sp strain NCIMB 12038, Appl. Environ. Microbiol. 63 (1997) 151–155.
[88] B.D. Erickson, F.J. Mondello, Nucleotide sequencing and transcriptional mapping of the genes encoding biphenyl dioxygenase, a multicomponent polychlorinated-biphenyl-degrading enzyme in *Pseudomonas* strain LB400, J. Bacteriol. 174 (1992) 2903–2912.
[89] K. Furukawa, T. Miyazaki, Cloning of a gene cluster encoding biphenyl and chlorobiphenyl degradation in *Pseudomonas pseudoalcaligenes*, J. Bacteriol. 166 (1986) 392–398.
[90] E. Masai, A. Yamada, J.M. Healy, T. Hatta, K. Kimbara, M. Fukuda, K. Yano, Characterization of biphenyl catabolic genes of gram-positive polychlorinated biphenyl degrader *Rhodococcus* sp. strain RHA1, Appl. Environ. Microbiol. 61 (1995) 2079–2085.
[91] D.T. Gibson, D.L. Cruden, J.D. Haddock, G.J. Zylstra, J.M. Brand, Oxidation of polychlorinated biphenyls by *Pseudomonas* sp. strain LB400 and *Pseudomonas pseudoalcaligenes* KF707, J. Bacteriol. 175 (1993) 4561–4564.
[92] F.J. Mondello, M.P. Turcich, J.H. Lobos, B.D. Erickson, Identification and modification of biphenyl dioxygenase sequences that determine the specificity of polychlorinated biphenyl degradation, Appl. Environ. Microbiol. 63 (1997) 3096–3103.
[93] D.T. Gibson, *Beijerinckia* sp strain B1: a strain by any other name, J. Ind. Microbiol. Biotechnol. 23 (1999) 284–293.
[94] E. Kim, G.J. Zylstra, Functional analysis of genes involved in biphenyl, naphthalene, phenanthrene, and *m*-xylene degradation by *Sphingomonas yanoikuyae* B1, J. Ind. Microbiol. Biotechnol. 23 (1999) 294–302.
[95] D.T. Gibson, V. Mahadevan, D.M. Jerina, H. Yogi, H.J. Yeh, Oxidation of the carcinogens benzo[*a*]pyrene and benzo[*a*]anthracene to dihydrodiols by a bacterium, Science 189 (1975) 295–297.
[96] G.J. Kleywegt, T.A. Jones, Detection, delineation, measurement and display of cavities in macromolecular structures, Acta Crystallogr. D Biol. Crystallogr. 50 (1994) 178–185.
[97] K. Furukawa, H. Suenaga, M. Goto, Biphenyl dioxygenases: functional versatilities and directed evolution, J. Bacteriol. 186 (2004) 5189–5196.
[98] J.V. Parales, R.E. Parales, S.M. Resnick, D.T. Gibson, Enzyme specificity of 2-nitrotoluene 2,3-dioxygenase from *Pseudomonas* sp. strain JS42 is determined by the C-terminal region of the alpha subunit of the oxygenase component, J. Bacteriol. 180 (1998) 1194–1199.

[99] R.E. Parales, M.D. Emig, N.A. Lynch, D.T. Gibson, Substrate specificities of hybrid naphthalene and 2,4-dinitrotoluene dioxygenase enzyme systems, J. Bacteriol. 180 (1998) 2337–2344.
[100] C. Bagneris, R. Cammack, J.R. Mason, Subtle difference between benzene and toluene dioxygenases of *Pseudomonas putida*, Appl. Environ. Microbiol. 71 (2005) 1570–1580.
[101] B.D. Ensley, B.J. Ratzkin, T.D. Osslund, M.J. Simon, L.P. Wackett, D.T. Gibson, Expression of naphthalene oxidation genes in *Escherichia coli* results in the biosynthesis of indigo, Science 222 (1983) 167–169.
[102] B.C. Buckland, S.W. Drew, N.C. Connors, M.M. Chartrain, C. Lee, P.M. Salmon, K. Gbewonyo, W. Zhou, P. Gailliot, R. Singhvi, R.C. Olewinski Jr., W.J. Sun, J. Reddy, J. Zhang, B.A. Jackey, C. Taylor, K.E. Goklen, B. Junker, R.L. Greasham, Microbial conversion of indene to indandiol: a key intermediate in the synthesis of CRIXIVAN, Metab. Eng. 1 (1999) 63–74.
[103] J. Reddy, C. Lee, M. Neeper, R. Greasham, J. Zhang, Development of a bioconversion process for production of *cis*-1*S*,2*R*-indandiol from indene by recombinant *Escherichia coli* constructs, Appl. Microbiol. Biotechnol. 51 (1999) 614–620.
[104] N. Zhang, B.G. Stewart, J.C. Moore, R.L. Greasham, D.K. Robinson, B.C. Buckland, C. Lee, Directed evolution of toluene dioxygenase from *Pseudomonas putida* for improved selectivity toward *cis*-indandiol during indene bioconversion, Metab. Eng. 2 (2000) 339–348.
[105] L.P. Wackett, Directed evolution of new enzymes and pathways for environmental biocatalysis, Ann. N. Y. Acad. Sci. 864 (1998) 142–152.
[106] W.L. DeLano, DeLano Scientific, San Carlos, CA, USA, 2000.